

## Monomer-dimer surface-reaction model: Influence of the dimer adsorption mechanism

M. Tammaro<sup>1</sup> and J. W. Evans<sup>2</sup>

<sup>1</sup>Ames Laboratory and Department of Physics, Iowa State University, Ames, Iowa 50011

<sup>2</sup>Ames Laboratory and Department of Mathematics, Iowa State University, Ames, Iowa 50011

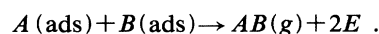
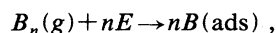
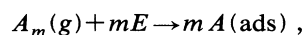
(Received 10 May 1995)

We consider the monomer-dimer surface reaction without surface diffusion for various dimer adsorption mechanisms, described below. After a dimer impinges “end on” at an empty site, its bottom atom remains there while its top atom searches  $N \geq 1$  sites, either in a *local* neighborhood ( $N$ -local models), or *randomly* located on the surface ( $N$ -random models), to find a second empty site. If one is found, the dimer can then adsorb dissociatively. The  $N$ -local models have a reactive window of finite width in the relative impingement rates, bordered by poisoning transitions, whereas the  $N$ -random models exhibit true bistability. As  $N$  increases, the reactivity is either strictly or effectively confined to relative impingement rates close to the stoichiometric ratio. We precisely analyze the limiting behavior as  $N \rightarrow \infty$ .

PACS number(s): 05.40.+j, 82.65.Jv, 82.20.Mj

### I. INTRODUCTION

It is instructive here to consider first a rather general class of surface reaction models [1], involving molecules  $A_m$  of  $m$   $A$  atoms and  $B_n$  of  $n$   $B$  atoms, which include the following steps:



Here  $(g)$  represents a molecule in the gas phase,  $(\text{ads})$  represents an adspecies, and  $E$  represents an empty adsorption site. We assume that  $A_m(g)$  impinges on the surface with rate  $P_A$  and  $B_n(g)$  with rate  $P_B$  and that these species dissociatively adsorb if they find appropriate ensembles of empty sites. We normalize  $P_A + P_B$  to unity. Adjacent adsorbed species of different types react to form  $AB(g)$  at rate  $k$ , which could be infinitesimal, finite, or infinite. In general, there may be adspecies mobility. For a steady state to exist, since the removal rates for species  $A$  and  $B$  are necessarily always equal, it follows that the adsorption rates for both species must also be equal. It is important to note here the following distinction. The impingement rate is the rate at which adsorption events are *attempted* (successful or not), while the adsorption rate is the rate of *successful* adsorption attempts multiplied by the number of atoms in the adsorbing molecule.

If  $m = n$  and both  $A_m(g)$  and  $B_m(g)$  adsorb randomly on identically shaped configurations of empty sites, then clearly the ratio of the adsorption rates for species  $A$  and  $B$  is exactly equal to the ratio of the impingement rates (independent of the statistics of the adlayer). Therefore a reactive steady state is only possible if  $P_A = P_B$ . If there is an imbalance in impingement rates, then the species with the higher impingement rate will poison the surface [2]. This behavior is well known for the monomer-monomer or  $A + B$  reaction model ( $m = n = 1$ ). Here it

is also known that no true steady state exists even when  $P_A = P_B$ , but that the system slowly poisons as domains of  $A(\text{ad})$  and  $B(\text{ad})$  grow in size [3,4]. The behavior is analogous to that of the two-dimensional (2D) Voter model [4]. Presumably poisoning also occurs when  $P_A = P_B$  for  $m = n > 1$ , except that the poisoned state will be a nontrivial jammed state incorporating empty sites, but no adsorption ensembles of  $m = n$  empty sites [2]. Also the kinetics of poisoning may differ from when  $m = n = 1$ , but will no doubt still be slow. In contrast, if one introduces symmetry-breaking cooperativity into the adsorption process, then in general the ratio of the adsorption rates will depend on the adlayer statistics. A reactive steady state can potentially be achieved for a range of  $P_A \neq P_B$  by adjustment of the adlayer-statistics. The width or extent of this reactive regime clearly vanishes as one “switches off” the cooperativity. A key question is then whether this width vanishes continuously or rather at a nontrivial “tricritical point” for some nonzero degree of cooperativity. Zhuo, Redner, and Park [5] studied a cooperative monomer-monomer reaction, where the adsorption rate of  $A(g)$  at empty sites with  $n$  neighboring  $A(\text{ads})$  is now given by  $r^n P_A$ , but  $B(g)$  adsorption remains random at rate  $P_B$ . They suggested the existence of a tricritical point at some  $r = r_c < 1$ , below the  $r = 1$  noncooperative limit [5].

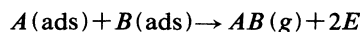
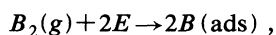
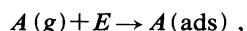
For  $m \neq n$ , invariably the ratio of adsorption rates for species  $A$  and  $B$  will depend on the adlayer statistics. Thus a reactive steady state can potentially be achieved for a range of  $P_A$ , again by suitable adjustment of the adlayer statistics. This is well known for the most intensively studied case of the monomer-dimer or  $A + B_2$  reaction model where  $m = 1$ ,  $n = 2$ , and  $B_2(g)$  adsorbs on adjacent pairs of empty sites [6,7]. Within the context of modifying the extent of reactivity, we comment on behavior in the reaction-limited regime as  $k \rightarrow 0$ . When  $k = 0+$ , the surface is completely covered. After each reactive removal of an adjacent  $AB$  pair, the created empty pair is immediately filled either by a single  $B_2(g)$  species or sequentially by two  $A(g)$  species. Clearly here

the adsorption rates are simply in proportion to the impingement rates [8,9] and are equal when  $P_A:P_B=1:4$ . In this case, the model exhibits slow poisoning due to coarsening of domains of  $A(\text{ad})$  and  $B(\text{ad})$ , analogous to the 2D Voter model, and the monomer-monomer model when  $P_A=P_B$  (see Ref. [4]). For the case of immobile adspecies, the reactive window narrows with decreasing  $k$  and was first proposed [9] to vanish at a nonzero tricritical value of  $k$ . However, more recent studies [4,10] suggest that its width vanishes continuously as  $k \rightarrow 0$ .

Here we consider the effect on the monomer-dimer or  $A+B_2$  reaction model of modifying the standard dimer adsorption mechanism. We consider only *immobile* adspecies and instantaneous reaction of adjacent  $AB$  pairs ( $k = \infty$ ). In the standard model, one randomly picks an empty site and then randomly selects *one* neighbor, adsorbing if it is also empty. In the modified models, we search for a second empty site among a local neighborhood of  $N \geq 1$  sites ( $N$ -local adsorption) or from among  $N \geq 1$  other randomly chosen sites on the lattice ( $N$ -random adsorption). In either case, as  $N \rightarrow \infty$ , a second empty site will certainly be found, so the adsorption rates for  $A(g):B_2(g)$  are in the proportion  $P_A:2P_B$ . Thus the steady-state reaction cannot be sustained if  $P_A \neq 2P_B$ , as  $N \rightarrow \infty$ . Here we provide a detailed analysis of the associated continuous decrease in the width of the reactive window for  $N$ -local models and of the continuous shrinkage of the regime of significant reactivity for  $N$ -random models, with increasing  $N$ .

## II. MODEL DESCRIPTIONS

The monomer-dimer surface reaction model



mimics CO oxidation on single crystal substrates, with  $A$  corresponding to CO and  $B_2$  to  $O_2$ . Here  $A(g)$  requires a single empty site to adsorb and  $B_2(g)$  requires an empty pair, which will not necessarily be adjacent in our prescriptions below. We assume that only adjacent  $AB$  pairs react and that this occurs instantaneously. Below we also set  $P_A=y$  and  $P_B=1-y$ . We shall consider only a square lattice of adsorption sites.

### A. $N$ -local adsorption

The dimer adsorption mechanism in these models can be described as follows. An empty site is chosen at random and then a local neighborhood of  $N$  sites is sampled in a fashion prescribed below, adsorption of  $B_2(g)$  occurring if at least one empty site is found in this neighborhood. For  $N=1$ , one nearest neighbor is chosen at random and our model corresponds to the standard Ziff-Gulari-Barshad (ZGB) monomer-dimer reaction model [6]. Next we discuss the case  $N=4$ . Here all four (hence  $N=4$ ) nearest neighbors of the first empty site are checked for vacancies. If any are found, then one is chosen randomly to accommodate the second  $B(\text{ad})$ . The

$N=1$  model is equivalent to randomly selecting adjacent pairs of empty sites, which might be thought of as dimer adsorption through a horizontal transition state. In contrast, the  $N=4$  model more reflects adsorption through a vertical transition state, where the lower end of the dimer attaches to an empty site (at least transiently), while the upper end searches for an empty neighbor. See Ref. [11].

Dimer adsorption in the  $N=8$  model proceeds as for  $N=4$ , but if a second empty adsorption site is *not* found in the first nearest neighbors, then the second nearest neighbors are checked for vacancy. If any are found, then one is chosen randomly from them. For the  $N=12$  model, if no vacancies are found among the first and second nearest neighbors, then the third nearest neighbors are checked and one is selected at random (if any are found). The next case in this sequence where one searches "shell by shell" for a second adsorption site is  $N=20$  because there are eight fourth-nearest neighbors on a square lattice [Fig. 1(a)]. Models for intermediate- $N$  values could also be considered, as well as various other prescriptions of neighborhoods and searching procedures.

For the  $N=1$  ZGB model, simulations have shown [12,13] that a reactive steady state exists only for  $y_1=0.3906 < y < y_2=0.5256$ . There is a continuous transition to a  $B$ -poisoned state as  $y$  decreases below  $y_1$  and a discontinuous transition to an  $A$ -poisoned state as  $y$  increases above  $y_2$ . These poisoned states, where every lattice site is occupied with  $A$  or  $B$ , are "adsorbing" since there is no spontaneous desorption of adatoms. One might expect this general picture to apply for  $N > 1$ , but that the location of these transitions shift and the width  $\Omega=y_2-y_1$  of the reactive window decreases with increasing  $N$ . We provide a detailed analysis of these trends in Sec. III, but first present some analytic results.

Because  $A(g)$  only needs a single empty site to adsorb, the (total) adsorption rate for  $A$  is  $Y_A(T)=yE$ , where  $E$  denotes the concentration of empty sites on the surface. The (total) adsorption rate for  $B$  is  $Y_B(T)=2(1-y)EQ$ , where  $Q$  is the conditional probability that if a single empty site is found, then another empty site will be found in the prescribed neighborhood of  $N$  sites. Note that  $Q$  depends only on the size  $N$  and on geometry of the neighborhood, but not on the order in which the sites are sampled. The presumably weaker dependence on this order will appear in the hierarchic rate equations for the probabilities for multisite configurations. Since the reaction mechanism guarantees that the removal rates of  $A$  and  $B$

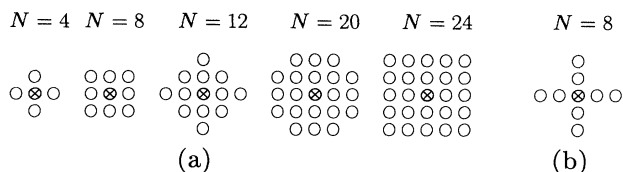


FIG. 1. (a) "Adsorption neighborhoods" in the  $N$ -local models for various  $N$ . If the center site (indicated by  $\otimes$ ) is empty, then the bottom  $B$  atom in the dimer lands there while the top  $B$  atom searches the other sites (indicated by  $\circ$ ) for a second vacancy. (b) An alternative geometry for the  $N=8$  model.

are equal, in a steady state, one must have  $Y_A(T) = Y_B(T)$ . This implies that either  $E = 0$  (poisoned state) or  $Q = y(1-y)^{-1}/2 \leq 1$ . Since the second condition cannot be satisfied for  $y > \frac{2}{3}$ , it follows that only poisoned states exist in this region. Furthermore, since trivially  $Y_A(T) > Y_B(T)$  for  $y > \frac{2}{3}$ , the system will always evolve to an  $A$ -poisoned state (unless initially  $B$  poisoned). Consequently, one has  $y_1 \leq y_2 \leq \frac{2}{3}$ .

Next consider evolution of the model through non-poisoned states for fixed  $y < \frac{2}{3}$ . Since  $Q \rightarrow 1$  as  $N \rightarrow \infty$ , it follows that  $Y_B(T) > Y_A(T)$ , so the system must evolve to a  $B$ -poisoned state. This implies that either  $y_1 \rightarrow \frac{2}{3}$  as  $N \rightarrow \infty$  or perhaps  $y_1$  remains below  $\frac{2}{3}$  as  $N \rightarrow \infty$  but the  $B$  coverage approaches unity (and the reaction rate vanishes) in the reactive steady state. In either case, one necessarily has  $y_2 \rightarrow \frac{2}{3}$  as  $N \rightarrow \infty$  and we shall see that the same is true for  $y_1$  (for this model).

### B. $N$ -random adsorption

Here the dimer adsorption mechanism is such that after a first empty site is selected randomly, one checks up to  $N$  other *randomly located* sites on the lattice and adsorbs the dimer if and when one of these is found to be empty. In this model, one has  $Y_A(T) = yE$  and  $Y_B(T) = 2(1-y)E[1 - (1-E)^N]$ . The latter quantity can be obtained exactly in contrast to the  $N$ -local adsorption model. Thus in a steady state, where these rates are equal, one has exactly

$$\frac{y}{2(1-y)} = 1 - (1-E)^N$$

(or  $E = 0$  for a poisoned state). This immediately shows that  $E \rightarrow 0$  continuously, as  $y \rightarrow 0$ , in the reactive steady state, so nontrivial continuous  $B$ -poisoning transitions cannot occur in this model and consequently  $y_1 = 0$  for all  $N$ . One might expect these models to support a discontinuous  $A$ -poisoning transition for  $y < \frac{2}{3}$ , as did the  $N$ -local adsorption models. However, below we shall see that instead they display true bistability for all  $N$ , i.e., for  $0 < y < y_s$  (a spinodal) a stable reactive steady state and stable  $A$ -poisoned state coexist. The stable  $A$ -poisoned state at  $y = 0$  is joined to the stable reactive state at  $y = y_s$  by an unstable steady-state branch to form a van der Waals type loop. For  $y > y_s$ , only the  $A$ -poisoned state is stable. In the  $N \rightarrow \infty$  limit, we again have  $Y_B(T) > Y_A(T)$  for  $y < \frac{2}{3}$ , so it is clear that  $y_s \rightarrow \frac{2}{3}$  and that the  $B$  coverage of the reactive steady state for any  $y < \frac{2}{3}$  must approach unity as  $N \rightarrow \infty$ .

## III. SIMULATION RESULTS FOR $N$ -LOCAL ADSORPTION MODELS

Our goal is a precise analysis of the vanishing width of the reactive window as  $N \rightarrow \infty$ . This is complicated both by the presence of a "long-lived" metastable reactive state just above the discontinuous transition [2,8,13] and by the presence of large fluctuations at the continuous transition [12], which could influence behavior across the entire (narrow) reactive window.

### A. The discontinuous transition: Constant-coverage analysis

We circumvent metastability problems by utilizing a constant-coverage kinetic ensemble [13] to locate the transition  $y_2$ . (The danger is that a conventional simulation will tend to overestimate  $y_2$  due to strong metastability [8].) In conventional simulations, a fixed value of  $y$  is chosen and  $[A]$  is monitored. In the constant-coverage ensemble, a fixed value of  $[A]$  is chosen, say,  $[A]_0$ . Whenever  $[A] < [A]_0$  an attempt at  $A$  adsorption is made and whenever  $[A] > [A]_0$  an attempt at  $B_2$  adsorption is made. One obtains  $y$  as the asymptotic fraction of  $A$  adsorption attempts to the total number of attempts. Since the value of  $[A]$  jumps from some typically small value (less than 0.1) to unity at the discontinuous transition, by choosing  $[A]_0 = 0.5$ , this guarantees that the associated  $y$  value will correspond to  $y_2$ . The results are shown in Table I. These runs were performed on a  $300 \times 300$  lattice for 100 000 time steps. Note that fluctuations in  $y$  are reduced for large  $N$ . Here dimer adsorption is effectively contingent on finding just one empty site, like monomer adsorption. Thus the situation is similar to the monomer-monomer model, where we also find very small fluctuations (about  $y = \frac{1}{2}$ ) in a constant-coverage simulation.

One may ask if there is a sizable dependence of the location of the transitions upon the particular geometry of the prescribed neighborhood of  $N$  sites. We determined the location of the discontinuous transition in the model for  $N = 8$  with a different geometry [nearest neighbors and third-nearest neighbors; see Fig. 1(b)] and found only a small variation (about 0.6%) from the location for the original  $N = 8$  geometry shown in Fig. 1(a).

### B. The continuous transition: Epidemic analysis

We determine the location of the continuous transition  $y_1$  by means of an epidemic analysis [12], wherein one monitors the evolution of an initially empty patch (in this case a single site) on an otherwise  $B$ -poisoned surface. We determined the "survival probability"  $P(t)$  that the patch has not become  $B$  poisoned at time  $t$  for various values of  $y$ .  $P(t)$  should saturate at a nonzero asymptotic value for  $y > y_1$ , where there is a finite probability of indefinite growth. However,  $P(t)$  should decrease ex-

TABLE I.  $N$ -local models. Discontinuous  $A$ -poisoning transition location  $y_2$ , determined using a constant-coverage analysis.

$N$	$y_2$	$\frac{2}{3} - y_2$
1	0.525 60	0.141 07
4	0.655 20	0.011 46
8	0.664 39	0.002 27
12	0.665 74	0.000 92
20	0.666 33	0.000 33
24	0.666 44	0.000 22
28	0.666 52	0.000 15
36	0.666 575	0.000 092
44	0.666 607 8	0.000 058 9

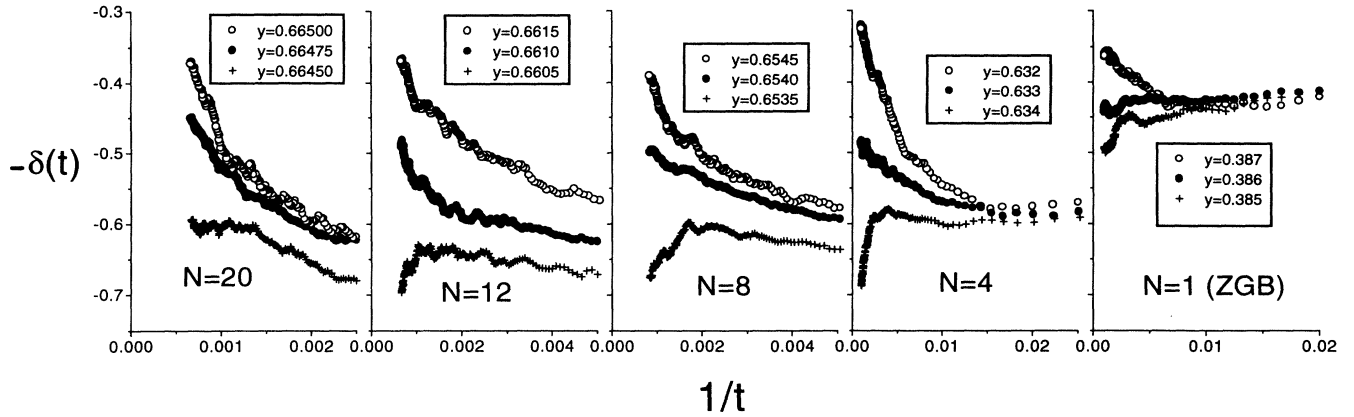


FIG. 2. Epidemic analysis of the survival probability  $P(t)$  for the  $N$ -local models. Plotted is the local slope  $-\delta(t)$  vs  $1/t$ . Here the transition  $y = y_1$  is determined from the requirement that  $\delta(t) \rightarrow 0.452$  as  $t \rightarrow \infty$ .

ponentially for  $y < y_1$ , where ultimate extinction is certain. However, at  $y_1$ , the survival probability is expected to scale like [12]  $P(t) \sim t^{-\delta}$ . For the ZGB model, analysis has shown [12] that this transition is in the universality class of Reggeon field theory (RFT), where  $\delta = 0.452 \pm 0.008$ . This is also expected to be the case for all  $N > 1$ .

Following Jensen, Fogedby, and Dickman [12], we examine the local slope

$$\delta(t) = \frac{\ln[P(t)/P(t/5)]}{\ln(5)}.$$

As  $t \rightarrow \infty$ , the local slope should curve upward (approaching zero) for  $y > y_1$  and it should curve downward (approaching  $-\infty$ ) for  $y < y_1$ . At  $y = y_1$ , the local slope should converge to the RFT value of  $\delta$ . The behavior of  $\delta(t)$  for  $N = 1, 4, 8, 12$ , and  $20$  is shown in Fig. 2 and the results are summarized in Table II. Note that if one writes [12]  $\delta(t) \sim 0.452 + a/t$  as  $t \rightarrow \infty$ , then  $a$  changes from a positive sign when  $N = 1$  and to a negative sign for all  $N > 1$ . Another quantity of interest is the average number of empty sites in the patch as a function of time  $N(t)$ . It is possible to perform an analysis identical to that for the survival probability [12]. At the transition, this quantity is expected to scale like  $N(t) \sim t^\eta$  with the RFT  $\eta = 0.224 \pm 0.010$ . The behavior for  $N = 12$  of the corresponding local slope  $\eta(t)$ , defined analogously to  $\delta(t)$ , is shown in Fig. 3 and is consistent with RFT. The survival probabilities were calculated using data averaged over 50 000–150 000 trials.

TABLE II.  $N$ -local models. Continuous  $B$ -poisoning transition location  $y_1$ , determined using an epidemic analysis, and the associated width of the reactive window obtained also using  $y_2$  values from Table I.

$N$	$y_1$	$y_2 - y_1$
1	0.391	0.135
4	0.633	0.022
8	0.654	0.011
12	0.6610	0.0048
20	0.66475	0.0016

### C. Scaling behavior

We now propose two scaling relations associated with the dependence of  $y_1$  and  $y_2$  on  $N$ . For the width of the reactive window  $\Omega = y_2 - y_1$ , if we assume that  $\Omega \sim N^{-\omega}$  for large  $N$ , then our data (Fig. 4) indicate that  $\omega = 2.1 \pm 0.5$ . For the distance of  $y_2$  from  $\frac{2}{3}$ ,  $\Delta = \frac{2}{3} - y_2$ , if we assume that  $\Delta \sim N^{-\lambda}$  for large  $N$ , then our data (Fig. 4) indicate that  $\lambda = 2.1 \pm 0.1$ .

## IV. SIMULATION RESULTS FOR $N$ -RANDOM ADSORPTION MODELS

As mentioned in Sec. III B, we find true bistability in this model. Results for the van der Waals type loops in the steady state  $[A]$  versus  $y$  are shown in Fig. 5 for  $N = 1, 2$ , and  $4$ . The stable branches can be determined using either a conventional or a constant-coverage simulation, but the unstable branches were necessarily found using a constant-coverage simulation. We further checked for bistability by preparing the system slightly

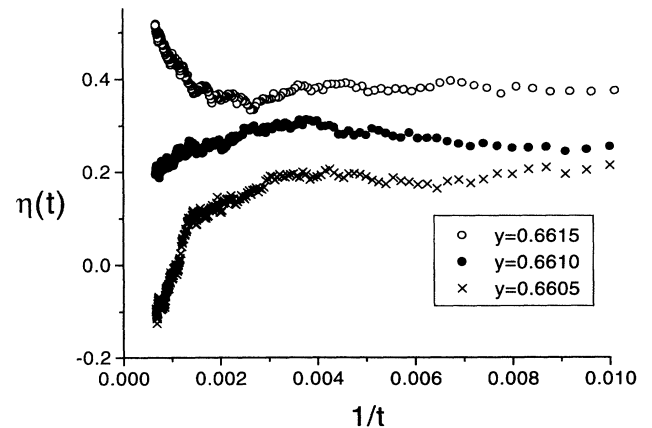


FIG. 3. Epidemic analysis of the average number of empty sites  $N(t)$  for the  $N$ -local model with  $N = 12$ . Plotted is the local slope  $\eta(t)$  vs  $1/t$ . Here the transition is determined from the requirement that  $\eta(t) \rightarrow 0.224$  as  $t \rightarrow \infty$ .

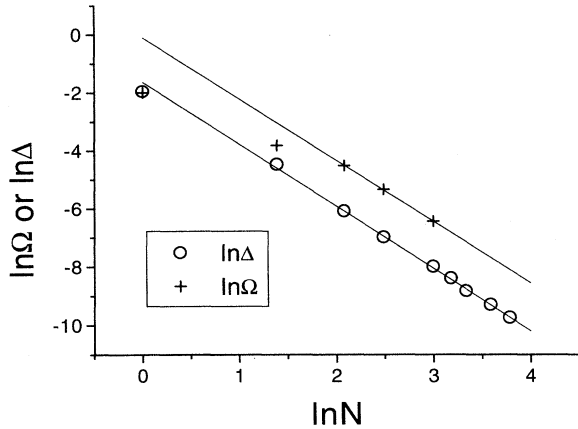


FIG. 4. Scaling analysis of the  $N$ -local model simulation results for  $\Delta = \frac{2}{3} - y_2$  and  $\Omega = y_2 - y_1$ .

above (below) the unstable branch and checking that it evolved to the poisoned (reactive) state. For the larger  $N$ ,  $[A]$  versus  $y$  near the spinodal approximates a vertical line, so the precise determination of  $y_s$  versus  $N$  is difficult. Thus, instead, we simply run the constant coverage simulation for  $[A]_0 = 0.5$  and show in Table III the convergence of the corresponding  $y = y([A]_0)$  values to  $\frac{2}{3}$  as  $N$  increases. If we assume that  $\Delta[A_0] \sim e^{-\mu N}$ , then fitting our data indicates that  $\mu = \mu[A_0] = 0.46 \pm 0.03$  for  $[A_0] = 0.5$ . This dependence is fundamentally different from behavior of transition locations in the  $N$ -local adsorption models and corresponds to mean-field-type behavior (see Sec. V). We note that fluctuations in  $y$  in the constant-coverage simulations are reduced for large  $N$  in the  $N$ -random model, just as in the

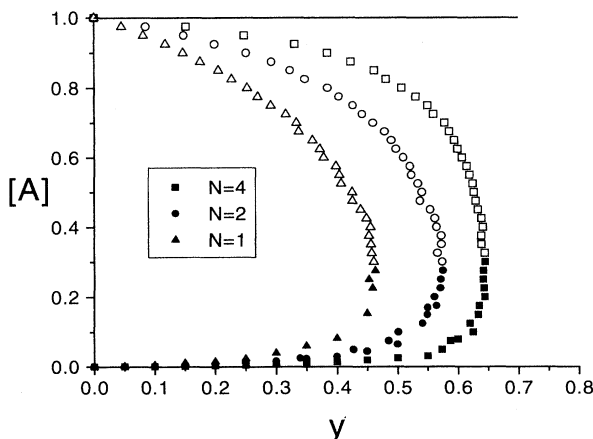


FIG. 5. "Phase diagram" for the  $N$ -random models determined by simulation. Plotted is the steady-state  $A$  coverage  $[A]$  vs the  $A(g)$ -impingement probability  $y$ . The open symbols indicate the unstable reactive steady-state branch, the solid symbols indicate the stable reactive steady-state branch, and the line  $[A] = 1$  gives the stable  $A$ -poisoned steady state (common to all  $N$ ).

TABLE III.  $N$ -random models. Behavior of  $y(A_0)$  for  $A_0 = 0.5$ .

$N$	$y(A_0 = 0.5)$	$\frac{2}{3} - y(A_0 = 0.5)$
1	0.428 12	0.238 54
2	0.547 84	0.118 83
4	0.627 40	0.039 26
8	0.661 17	0.005 49
12	0.665 81	0.000 86
16	0.666 534	0.000 133
20	0.666 643 4	0.000 023 3

$N$ -local model. However, we find somewhat stronger finite-size effects in the  $N$ -random model:  $y[A_0]$  values decrease with increasing system size [e.g., by  $O(10^{-3})$  changing from a  $500 \times 500$  to a  $1000 \times 1000$  lattice].

It is appropriate to comment on why these models display true bistability, rather than a discontinuous  $A$ -poisoning transition, for all  $N$ . To this end, one might consider another class of dimer adsorption mechanisms where after the first empty site is selected, one checks  $N$  others randomly located within a distance  $L$  of the first site. For finite  $L$ , one again expects to find a discontinuous transition. However, presumably  $L$  determines the critical size of a nucleus of the stable poisoned (reactive) state embedded in the metastable reactive (poisoned) state for impingement rates  $y$  above (below) the transition. Thus as  $L$  increases (for fixed  $N$ ), so does the critical size and thus so does the lifetime of the metastable state.

## V. MEAN-FIELD THEORY

We now present a rate equation analysis for both models in the mean-field site approximation. Here all spatial correlations are neglected, so multisite configuration probabilities simply factorized into products of site probabilities. However, the infinite reaction rate and the unusual dimer adsorption mechanism in the  $N$ -local model cause some complications. In this discussion, let  $A$  ( $B$ ) also represent the coverage or concentration of  $A$  ( $B$ ) on the surface, and let  $E$  represent the fraction of empty sites. For both species  $J = A$  and  $B$ , it is convenient to introduce rates for nonreactive (NR) adsorption  $Y_J(\text{NR})$  and reactive (R) adsorption (adsorption followed by instantaneous reaction)  $Y_J(\text{R})$ , as well as the previously discussed total ( $T$ ) adsorption rates  $Y_J(T) = Y_J(\text{NR}) + Y_J(\text{R})$ . Then the rate equations (for infinite reaction rate) have the form [14,15]

$$\frac{dA}{dt} = Y_A(\text{NR}) - Y_B(\text{R}) = Y_A(\text{NR}) + Y_B(\text{NR}) - Y_B(T),$$

$$\frac{dB}{dt} = Y_B(\text{NR}) - Y_A(\text{R}) = Y_A(\text{NR}) + Y_B(\text{NR}) - Y_A(T).$$

In a steady state, one has  $dA/dt = dB/dt = 0$  providing a set of coupled nonlinear algebraic equations for  $A$  and  $B$  (noting that  $A + B + E = 1$ ).

For the  $Y_A$ 's, in both the  $N$ -local and  $N$ -random adsorption models, we have

$$Y_A(T) = yE, \quad Y_A(\text{NR}) = yE(1-B)^4.$$

The first result is exact (as noted previously) and the second simply accounts for the fact that nonreactive  $A$  adsorption requires that none of the four neighbors of the adsorption site be occupied by  $B$  [producing an extra factor of  $(1-B)^4$  in the site approximation]. Next consider the  $Y_B$ 's. In both models, we have

$$Y_B(T) = 2(1-y)E[1-(1-E)^N].$$

This expression is exact for  $N$ -random adsorption, as noted above. Clearly there are two contributions to the filling of an empty site by  $B$ : *direct* adsorption where the site is selected first by the "bottom atom" in the depositing dimer and *indirect* adsorption where the site is selected by the "top atom" in the dimer as a result of searching  $N$  other sites. Clearly, both contributions to  $Y_B(T)$  are equal. However, for  $Y_B(\text{NR})$ , the behavior is model specific, as detailed below.

$$\begin{aligned} \delta Y_B(\text{NRD}) &= (1-y)E[(1-A)^4 - B^4] \text{ for the first shell} \\ &= (1-y)EB^4[1-(1-E)^4] \text{ for the second shell} \\ &= (1-y)EB^4(1-E)^4[1-(1-E)^4] \text{ for the third shell,} \end{aligned}$$

etc. The first-shell contribution accounts for the requirement that no first-shell sites can be occupied by  $A$ , but also that they cannot all be occupied by  $B$ . For second-shell adsorption, all first-shell sites must be occupied by  $B$  and at least one second-shell site must be empty, etc. Similarly, we obtain

$$\begin{aligned} \delta Y_B(\text{NRI}) &= (1-y)E(1-A)^3[1-(1-E)^4] \text{ for the first shell} \\ &= (1-y)E(1-E)^2B^2(1-A)^2[1-(1-E)^4] \text{ for the second shell} \\ &= (1-y)E(1-E)^7B(1-A)^3[1-(1-E)^4] \text{ for the third shell,} \end{aligned}$$

etc. For the first-shell contribution, one requires the indirectly filled site of interest to be empty, one of its four neighbors (the direct adsorption site) to be empty, and the other three not be filled by  $A$  (denoted by  $A'$  in Fig. 6). One then sums over all possible states of the other three sites (denoted by an asterisk in Fig. 6) neighboring the direct adsorption site, weighting by the probability that the top atom selects the empty site of interest to fill indirectly. Performing this sum (see Fig. 6) yields the above expression, which can also be understood as follows. Pick the site of interest to be filled indirectly. As noted above, one of the four neighbors must be the direct adsorption site and must be empty, contributing a factor

$$\begin{array}{c} A' \quad * \\ A' \quad E \quad E \quad * \\ A' \quad * \end{array} \quad \delta Y_B(\text{NRI}) = 4A'^3E^2 \sum_{m=0}^3 \frac{1}{m+1} \binom{3}{m} E^m (1-E)^{3-m}$$

FIG. 6. Determination of the first-shell contribution to  $\delta Y_B(\text{NRI})$ . The direct (indirect) adsorption site is the empty site on the right (left). The sum determines the *indirect*  $B$ -adsorption rate on the left  $E$  site, accounting for all possible configurations of the  $*$  sites. If  $m$  of these are  $E$ , and thus  $3-m$  are  $A$  or  $B$ , the probability that indirect adsorption occurs on the left  $E$  site is  $1/(m+1)$ . Here  $A'$  means "not"  $A$ .

### A. Analysis of $N$ local adsorption models

First we consider separately the case  $N=1$  (the ZGB model), where direct and indirect contributions to  $Y_B(\text{NR})$  are equal. Here it has been shown that [14,15]

$$Y_B(\text{NR}) = 2(1-y)E^2(1-A)^3,$$

which is proportional to the probability of finding an empty site (accommodating the bottom  $B$  atom) surrounded by an empty site (accommodating the top  $B$  atom) and three non- $A$  sites (thus avoiding reaction of the bottom  $B$  atom).

In the  $N$ -local model for general  $N$  corresponding to some specific number of "shells" ( $N=4, 8, 12, \dots$ ), our chosen search algorithm allows us to sum cumulatively contributions to  $Y_B(\text{NR})$  from each shell, but necessarily separating distinct contributions from *direct* [ $\delta Y_B(\text{NRD})$ ] and *indirect* [ $\delta Y_B(\text{NRI})$ ] adsorption. We thus obtain

of  $4E$ ; the other neighbors cannot be occupied by  $A$ , contributing a factor of  $(1-A)^3$ . In order for the top  $B$  atom to land, at least one of the neighbors of the direct adsorption site must be empty, contributing a factor  $\{1-(1-E)^4\}$ . There is a probability of  $\frac{1}{4}$  that this neighbor is the site of interest. Contributions to  $Y_B$  from indirect filling of other shells can be understood similarly.

Figure 7(a) shows mean-field predictions for the steady state  $[A]$  versus  $y$ , for three  $N$  values, using above expressions for adsorption rates. These predict qualitatively correct behavior, apart from the expected absence of a continuous  $B$  poisoning. The location of the spinodals in the  $N=1$  (ZGB),  $N=4$ , and  $N=8$  models are  $y_s = 0.561\,012$  (cf. Ref. [14]),  $0.663\,667$ , and  $0.666\,629$ , respectively.

### B. Analysis of $N$ random adsorption models

For dimer adsorption on an infinite lattice, the two  $B$ 's will land on infinitely separated randomly selected sites. Clearly the probability that either will react is the same and therefore the direct and indirect contributions to  $Y_B$  are equal. The only difference from the total rate is that we must multiply by the probability that there are no  $A$ 's on the four nearest neighbors of the adsorbed  $B$ . There-

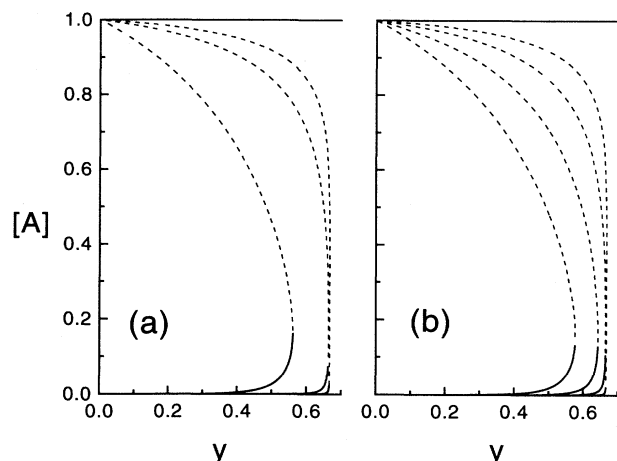


FIG. 7. Mean-field "phase diagrams." Plotted are the steady-state  $A$  coverage  $[A]$  vs the  $A(g)$ -impingement probability  $y$ . (a)  $N$ -local models for  $N=1, 4$ , and  $8$ . (b)  $N$ -random models for  $N=1, 2, 4$ , and  $8$ .

fore the nonreactive rate for the  $B$  is

$$Y_B(\text{NR}) = 2(1-y)E[1-(1-E)^N](1-A)^4.$$

Figure 7(b) shows mean-field predictions for the steady state  $[A]$  versus  $y$  for three  $N$  values, using the above expressions for adsorption rates. Qualitatively correct behavior is predicted. The values for the spinodals are  $y_s = 0.57691, 0.64253, 0.66437$ , and  $0.6666433$  for  $N=1, 2, 4$ , and  $8$ , respectively.

### C. Asymptotic behavior for large $N$

Now we will show that mean-field predictions for the spinodal location (in both models) have a deviation from  $\frac{2}{3}$  that decreases exponentially with  $N$ . It is convenient to analyze the behavior of  $y$  for fixed  $A = A_0$ , with corresponding  $E = E_0$ . Since  $Y_A(T) = Y_B(T)$ , one has

$$y \cong \frac{2}{3} [1 - \frac{1}{3}(1-E_0)^N]$$

for large  $N$  and  $0 < E_0 < 1$ . Then, solving for  $\Delta = \frac{2}{3} - y$ , we have  $\Delta \sim e^{-\mu N}$  as  $N \rightarrow \infty$ , where  $\mu = -\ln(1-E_0) > 0$ .

Thus we have exponential decay provided  $0 < E_0 < 1$ , which presumably applies to the spinodal. Furthermore, for the  $N$ -random model, we can obtain simply an exact expression for the decay rate. In the steady state here, we have

$$\begin{aligned} \frac{dA}{dt} &= yE(A+E)^4 \\ &+ 2(1-y)E[1-(1-E)^N][(1-A)^4-1] = 0. \end{aligned}$$

Letting  $N \rightarrow \infty$  and  $y \rightarrow \frac{2}{3}$ , we have for the steady state

$$(A_0 + E_0)^4 = 1 - (1 - A_0),$$

which has a solution  $E_0$ , satisfying  $0 < E_0 < 1$ , for any  $A_0$  between zero and one. Solving for  $1 - E_0$ , we obtain

$$\mu = -\ln\{1 + A_0 - [1 - (1 - A_0)^4]^{1/4}\}.$$

The maximum decay rate, corresponding to the spinodal, occurs at  $A_0 = 1 - 2^{-1/4} \approx 0.159$ , yielding  $\mu = -\ln(2 - 2^{3/4}) \approx 1.145$ .

## VI. CONCLUSIONS

We have provided a detailed analysis of the influence of the dimer adsorption mechanism on reactivity in the diffusionless monomer-dimer surface reaction model. First, we let the dimer sample  $N$  sites in a *local* neighborhood of a randomly selected empty site in order to find a second empty site allowing adsorption. We find that the width of the reactive window between poisoning transitions decreases continuously like  $N^{-2.1 \pm 0.5}$  and shifts towards the stoichiometric value of the relative impingement rates ( $y = \frac{2}{3}$ ) like  $N^{-2.1 \pm 0.1}$ . Instead, letting the dimer sample  $N$  other *randomly* chosen sites produces true bistability. Now the spinodal approaches  $y = \frac{2}{3}$  exponentially, corresponding to mean-field-type behavior.

## ACKNOWLEDGMENTS

This work is supported by the Division of Chemical Sciences, Office of Basic Energy Sciences of the U.S. Department of Energy (DOE). Ames Laboratory is operated for the U.S. DOE by Iowa State University under Contract No. W-7405-Eng-82.

- [1] V. I. Bykov, V. I. Elokhin, and G. S. Yablonskii, *React. Kin. Catal. Lett.* **4**, 191 (1976); V. I. Bykov, G. A. Chumankov, V. I. Elokhin, and G. S. Yablonskii, *ibid.* **4**, 397 (1976).
- [2] J. W. Evans, *Langmuir* **7**, 2514 (1991).
- [3] E. Wicke, P. Kummann, W. Keil, and J. Schiefeler, *Ber. Bunsenges. Phys. Chem.* **84**, 315 (1980); R. M. Ziff and K. Fichthorn, *Phys. Rev. B* **34**, 2038 (1986); D. ben-Avraham, S. Redner, D. B. Considine, and P. Meakin, *J. Phys. A* **23**, L613 (1990); D. ben-Avraham, D. Considine, P. Meakin, S. Redner, and H. Takayasu, *ibid.* **23**, 4297 (1990); P. L.

- Krapivsky, *Phys. Rev. A* **45**, 1067 (1992); E. Clement, P. Leroux-Hugon, and L. M. Sander, *Phys. Rev. Lett.* **67**, 1661 (1991); *J. Stat. Phys.* **65**, 925 (1991).
- [4] J. W. Evans and T. R. Ray, *Phys. Rev. E* **47**, 1018 (1993).
- [5] J. Zhuo, S. Redner, and H. Park, *J. Phys. A* **26**, 4197 (1993).
- [6] R. M. Ziff, E. Gulari, and Y. Barshad, *Phys. Rev. Lett.* **56**, 2553 (1986).
- [7] M. Dumont, P. Dufour, B. Sente, and R. Dagonnier, *J. Catal.* **122**, 95 (1990).
- [8] J. W. Evans and M. S. Miesch, *Phys. Rev. Lett.* **66**, 833

- (1991).
- [9] D. Considine, H. Takayasu, and S. Redner, *J. Phys. A* **23**, L1181 (1990).
- [10] J. Kohler and D. ben-Avraham, *J. Phys. A* **25**, L141 (1992).
- [11] R. S. Nord and J. W. Evans, *J. Chem. Phys.* **93**, 8397 (1990).
- [12] I. Jensen, H. C. Fogedby, and R. Dickman, *Phys. Rev. A* **41**, 3411 (1990).
- [13] R. M. Ziff and B. Brosilow, *Phys. Rev. A* **46**, 4630 (1992).
- [14] R. Dickman, *Phys. Rev. A* **34**, 4246 (1986).
- [15] J. W. Evans and M. S. Miesch, *Surf. Sci.* **245**, 401 (1991).